# Effective Flow Control on Self-similar Traffic in ATM Networks- An FIR Neural Network Approach

*Yen Chieh Ouyang, Cheng Lun Sun and Wei Shi Lian*

Department of Electrical Engineering
National Chung Hsing University
Taichung, Taiwan 40227
Email: ycouyang@nchu.edu.tw

**ABSTRACT**

This work presents a novel feedback rate regulator using the multiple leaky bucket (MLB) for VBR self-similar traffic that is based on the traffic load prediction by time-delayed neural networks in ATM networks. In contrast to the conventional leaky bucket (LB), the leak rate and buffer capacity of all LBs are shared in the same virtual path to more effectively utilize network resources. In the MLB mechanism, the leak rate and buffer capacity of each LB can be dynamically adjusted based on the buffer occupancy. A finite-duration impulse response (FIR) multilayer neural network is used to predict the incoming traffic load and pass the information to the feedback rate regulator. In addition, ten real world MPEG1 and ten synthesized traffic traces are used to validate the performance of the MLB and the MLB with FIR prediction mechanism. Simulation results demonstrate that the cell loss rate using MLB and MLB with FIR has a three to more than ten thousand time improvement over the conventional leaky bucket method.

Keywords: Self-similar, ATM Networks, Multiple Leaky Bucket, Neural Networks, Traffic Control.

## 1. Introduction

ATM technology is based on a small and fixed size packet called a cell. These cells permit sufficiently rapid switching so that multiple isochronous data can be statistically multiplexed and physical resources can be maximally utilized. To maintain the quality of service (QoS) perceived by network users, the users must make contracts with networks. According to the contracts, a policing mechanism acts accordingly to protect all well-behaving sources. In ATM networks, the need for multimedia and real-time applications has increased rapidly. To elucidate the characteristics of these traffic, some rate regulators based on neural networks have been proposed [1, 2]. These mechanisms can increase bandwidth utilization and decrease cell loss rate while integrated with the rate-based feedback control scheme. Therefore, developing a simple and feasible feedback rate regulator for real-time services is of priority concern.

Many investigations have employed the leaky bucket control scheme to resolve a flow control problem [3, 4, 5, 6], while several policing mechanisms have been proposed as well [7, 8]. Actually, determining an appropriate leak rate and buffer capacity for a leaky bucket is a relatively difficult task. For an MPEG traffic source, it may generate cells at a near-peak rate for a short time interval and, immediately thereafter, become silent. Selecting a leak rate close to the source's peak rate may waste the bandwidth. In contrast, the cell loss rate (CLR) may be extremely high if a leak rate is close to the source's mean rate. As generally known, the cell loss rate can be reduced by increasing the buffer capacity. However, if the leak rate is too low, the cell loss rate cannot be greatly improved by merely increasing buffer capacity.

In light of above developments, we devised a source rate regulator (SRR) by using an FIR multilayer neural network to predict the incoming traffic load [9] and by adopting the concept of reactive congestion control. The weakness of reactive congestion control comes from high bandwidth-delay product, but its still valid when the control method is applied to monitor a single MPEG traffic as well as multiple self-similar traffics.

The rest of this paper is organized as follows. In section 2, the operation of FIR and its learning algorithm are summarized. Section 3 describes the characteristics of self-similar traffic. Section 4 discusses the leaky bucket mechanism and its modifications. In section 5, we present a novel policing mechanism called multiple leaky buckets (MLB) for controlling the self-similar traffic. To validate the performance of MLB, ten real-world MPEG1 video traces and synthesized self-similar traffic are used. Finally, conclusions and areas for future research are made in Section 6.

## 2. The FIR Multilayer Network

The multilayer feed-forward neural networks are extensively used in many areas, such as pattern recognition, character segmentation, or diagonsis. However, a major limitation of the standard multilayer neural network is that it can only learn an input-output mapping that is static [10]. The form of static input-output mapping is well suited for spatial application, but is inadequate for temporal application such as in time series prediction. By replicating hidden neurons and output neurons through time, the network is appropriate to be used in temporal applications [10]. This kind of neural network is called time-delay neural network (TDNN) [11]. The TDNN topology is embodied in a multilayer network in which each synapse is represented by a finite-duration impulse response (FIR) filter, as shown in Fig. 1. The weight $w_{ji}$

connected to the fixed input $x_0$ = -1 represents the threshold value.

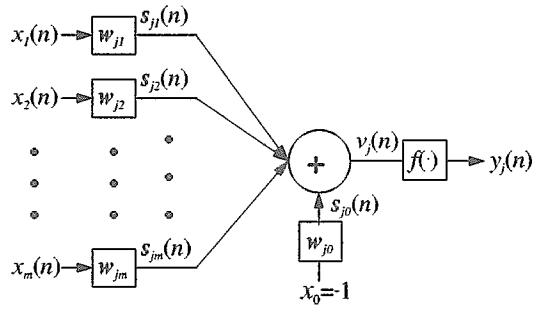


Figure 1 Spatial-temporal model of a neuron, incorporating synaptic FIR filter.

The FIR multilayer network is a feed-forward neural network whose hidden neurons and output neurons are replicated across finite duration of time. The temporal backpropagation learning algorithm is summarized as follows [11]:

$$w_{ij}(n+1) = w_{ij}(n) + \eta\, \delta_i(n) x_j(n) \qquad (1)$$

$$\delta_i(n) = \begin{cases} e_i(n) \cdot f\,(v_i(n)) & \text{if neuron } i \text{ is in the output layer} \\ f\,(v_i(n)) \cdot \sum_{q \in \Psi} \sum_{n=0}^{M} \delta_q(n+\chi) \cdot w_{qi}(n) & \text{if neuron } i \text{ is in a hidden layer} \end{cases}$$

where $w_{ij}$ represents the connection weight, $\eta$ represents the learning rate, $e_i$ is the difference between the desired output the neural network output, $f(\cdot)$ represents the activation function, $M$ represents the number of taps in the current layer, and $\Psi$ is the set of all neurons whose inputs are fed by neuron $i$ in (2) a feedforward manner. The FIR algorithm is composed of two phases: the off-line learning phase and the on-line processing phase. The off-line learning phase is mainly for training the FIR multilayer network, and is not used for predicting the number of incoming cells at the next period. Once the off-line learning phase is finished, the on-line processing phase begins. In the on-line processing phase, the FIR multilayer network is used to predict the number of incoming cells in the next period, and the cell discarding function is implemented based on the information provided by the FIR multilayer network. Note that when the accumulated prediction error is greater than a threshold value $\varepsilon$, the FIR multilayer network has to be trained again.

To train the FIR multilayer network in the off-line learning phase, we can collect the actual number of incoming cells in the first $K$ periods as the training data set. The training data set ($TDS$) is expressed as $TDS(1,K) = \{ G(1), G(2), \cdots, G(K) \}$.

Since there are no rules about how to properly design the topology of the FIR multilayer neural network for a specific problem, different topologies of FIR network are trained by using the training set $TDS(1,K)$. The network with the smallest accumulated error is chosen for performing prediction in the on-line processing phase. The accumulated error should be smaller than $\varepsilon$, or using bigger network for training. Note that in the off-line learning phase, the learning rate $\eta$ in (1) may potentially affect the converge speed of the training process. For a multilayer neural networks, the speed of the weight update in earlier iterations is faster than that of in latter iterations, therefore we can put a large value $\eta$ at the beginning of the training process and then replaced it with a smaller value after a large number of training iterations.

In the on-line processing phase, the trained FIR multilayer network is used to predict the number of incoming cells in the next period. If the predicted number of incoming cells in the next period does not exceed the buffer capacity, then all the incoming cells during the next period are admitted to enter the buffer. Note that it is possible that although the FIR multilayer network predicts no overflow for the next period, the overflow does happen at the next time slot. Under this circumstance, the feedback traffic rate regulator is used to adjust the source cell rate.

## 3. Characteristics of self-similar traffic

Most pertinent studies since 1993 [12, 13] have conferred that self-similar processes in real-world networking applications aptly describe traffic patterns. For example, Ethernet traffic, World Wide Web (WWW) traffic, and video traffic transmitted over ATM networks are self-similar. Recent studies also indicate that the self-similar traffic profoundly influences network performance [12, 13, 14, 15, 16, 17]. In the following sections, we introduce the definition, measurement, and major characteristics of self-similar traffic.

The Norros effective bandwidth formula can be utilized to estimate the bandwidth requirement for the coming traffic. The fact that most traffic patterns have self-similarity accounts for why developing an effective bandwidth formula for self-similar traffic is an essential task. Ilkka Norros [18] performed this task in an earlier investigation. Assume that the self-similar traffic source is given along with the mean bit rate $m$ (in bits/sec), the Hurst parameter $H$, and the variance coefficient $a$ (in bit-sec). The variance coefficient is the ratio of the variance (in bit-bit) over one second interval to the mean bit rate of the traffic stream.

For a given buffer size $B$ and desired cell loss ratio $\varepsilon$, the effective bandwidth $C$ of a self-similar traffic can be expressed as:

$$C = m + (k(H)\sqrt{-2\ln\varepsilon})^{1/H} a^{1/2H} B^{(H-1/H)} m^{1/2H} \qquad (3)$$

where $k(H) = H^H (1-H)^{(1-H)}$.

In sum, the Norros formula can be employed to estimate the effective bandwidth requirement for self-similar traffic. According to the Norros formula, the relationship among the bandwidth requirement, buffer capacity, desired cell loss rate, and related parameters for self-similar traffic can be derived. In [13], it demonstrated that a VBR video source transmitted over ATM networks is self-similar traffic. By using the

Norros formula, the network resource requirement for VBR video traffic can be estimated.

## 4. Feedback rate regulator for self-similar VBR traffic

This section introduces a novel rate-based feedback controller for self-similar VBR traffic in ATM networks. A multiple leaky buckets (MLB) mechanism is used to discard cells when a traffic contract is violated. When a possible discard is detected, the network element or switch generates a backward RM-cell and sets a congestion notification (CI) bit. When the source receives that backward RM-cell, the source rate must be throttled down. The higher the frequency of receiving the backward RM-cell implies a higher likelihood of discarding a cell and, subsequently, the higher the likelihood that the traffic is regulated at a lower rate. The following sections thoroughly describe the MLB mechanism and feedback control scheme.

### A. Multiple leaky buckets

In ATM networks, each virtual path (VP) may contain several traffic sources. Therefore, several independent leaky buckets may be available that monitor every traffic source. If these leaky buckets from all sources collaborate with each other, the bandwidth and buffer spaces can be effectively used, thereby reducing the cell loss rate (CLR) significantly.

Ho [20] first proposed the above notion and applied it to a policing mechanism which implements the CLB. CLB differs from LB mainly in that if a leaky bucket becomes empty, its leak rate is distributed to other buckets. To elevate the performance of CLB, our results indicate that there is no need to distribute leak rate to other buckets unless its buffer becomes empty. Besides, the LB could not only share the leak rate, but also share the buffer capacity.

However, when all the leaky buckets in the same VP are integrated, how to distribute the total leak rates and buffer spaces to each source is of relevant concern. Herein, we dynamically adjust the leak rate and buffer capacity for each LB according to their buffer occupancies.

Assume that there are $n$ traffic sources and $n$ leaky buckets for each LB that monitor one traffic source. The $i$th traffic source and LB have the following associative parameters:

- $M_i$ : the negotiated mean cell rate of $i$th traffic source (in cell/sec),
- $P_i$ : the negotiated peak cell rate of $i$th traffic source (in cell/sec),
- $R_i(t)$ : the leak rate of $i$th LB at time $t$ (in cell/sec),
- $B_i(t)$ : the buffer capacity of $i$th LB at time $t$ (in cell),
- $R_i(0)$ : the initial value of $R_i(t)$ (in cell/sec),
- $B_i(0)$ : the initial value of $B_i(t)$ (in cell),
- $K_i(t)$ : the number of cells in the $i$th buffer at time $t$,
- $O_i(t)$:the occupancy of $i$th buffer and $O_i(t) = K_i(t) / B_i(t)$,
- $\varepsilon$ : the desired cell loss rate

First, the initial values of the leak rate, $R_i(0)$, and buffer capacity, $B_i(0)$, must be determined, where $R_i(0)$ and $B_i(0)$ can be expressed as

$$R_i(0) = \gamma \cdot M_i \tag{4}$$

$$B_i(0) = \beta \cdot P_i \tag{5}$$

where $\gamma$ and $\beta$ are constant. The aggregate leaky rate and buffer capacity are denoted by $R_0$ and $B_0$ respectively, where $R_0$ is defined as

$$R_0 = \sum_{i=1}^{n} R_i(0) \tag{6}$$

and $B_0$ is defined as

$$B_0 = \sum_{i=1}^{n} B_i(0) \tag{7}$$

The time interval is denoted by $\Delta T$. After the initial values of the related parameters have been settled, the policing function must obtain the value for the buffer occupancy $O_i(t)$ every $\Delta T$ seconds. From $O_i(t)$, the new leak rate and new buffer capacity can be calculated. The new leak rate of $i$th LB is defined as follows:

$$R_i(t+1) = R_0 \cdot \frac{R_i(0) \cdot O_i(t)}{\sum_{i=1}^{n} R_i(0) \cdot O_i(t)} \tag{8}$$

Assume that the buffer spaces are shared. Thus, we define the reservation ratio, $\delta$, for each LB. Whereas $\delta$ can be expressed as

$$\delta = \frac{\textit{reserved buffer size}}{\textit{total buffer size}} \tag{9}$$

The $\delta$ used in FIR multilayer neural networks can be express as

$$\delta' = \frac{\textit{reserved buffer size}}{\textit{total buffer size}} \cdot (1 + (C_r / T_r)) \tag{10}$$

Where $Cr$ is the cell loss number and the $Tr$ is the total cell transmitted number.

Clearly, a situation in which the reserved part is too large implies that the benefit incurred from buffer sharing no longer exists. In contrast, if the reserved part is insufficient and if the source transmission rate is close to the peak rate, then buffer may quickly become full, resulting in a large number of cells being discarded. The new buffer capacity of $i$th LB should be defined as:

$$B_i(t+1) = (1-\delta') \cdot B_0 \cdot \frac{B_i(t) \cdot O_i(t)}{\sum_{i=1}^{n} B_i(t) \cdot O_i(t)} + \delta' B_i(0) \tag{11}$$

where the occupancy $O_i(t)$ is an indicator. If $O_i(t)$ exceeds the average value, $\frac{1}{n}\sum_{j=1}^{n} O_j(t)$, then the leak rate, $R_i(t)$, and buffer capacity, $B_i(t)$, are reassigned

higher values than their initial ones.

This mechanism is advantageous in that it can effectively distribute the leak rate and buffer capacity to reduce the CLR. If the counter is close to the maximum allowable value, cell loss would likely occur. In addition, increasing the leak rate and buffer capacity before cell loss occurs can markedly reduce the CLR..

### B. Multiple leaky buckets with feedback control

Feedback traffic control is used to reduce cell loss rate by regulating source transmission rate and provide better protection to well-behaving sources. The ATM traffic control model using a source rate regulator with FIR multilayer neural networks is shown in figure 2.

The main purpose of using feedback control is to reduce cell loss rate by regulating the source transmission rate and providing better protection to well-behaving sources. The difficult problem in preventive congestion control is choosing the right set of parameters to describe a source and allocate an appropriate amount of resources for it. In practice, if several sources generate data at their near-peak rate simultaneously, cell loss may still occur. In order to reduce the possibility that many sources request a large amount of resources during the same time period, use of the policing mechanism to control the source rate becomes essential.

To regulate the transmission rate, we defined an initial threshold value of $i$th traffic, denoted by $\theta_i(0)$. The new threshold value of $i$th traffic source, $\theta_i(t)$, is renewed every $\Delta T$ seconds and defined as:

$$\theta_i(t) = \frac{\theta_i(0)}{\max\{V_{m,i}(t), 1\}} \tag{12}$$

In addition, rate regulation can be employed to protect well-behaving sources. It is feasible to reduce the transmission rate for a malicious user that violates the contract. A modified version of feedback traffic regulation proposed in [1] was employed. The parameters of LBs are controlled by resource controller (RC). The RC catches the status of each LB in every $\Delta T$ seconds and calculates the new leaky rates, new buffer space and new threshold values from equations (14), (15) and (16), respectively. The objective of the source rate regulator (SRR) is to decide whether or not to throttle down the source transmission rate. When the occupancy of $i$th buffer, $O_i(t)$, exceeds its threshold value, $\theta_i(t)$ the SRR generates a backward RM-cell in which the congestion notification (CI) field is set to 1, and transmits it to source $i$. When the source $i$ receives a RM-cell with CI=1, it decreases its transmission rate by multiplying the factor $\omega_i(t)$, which is given by:

$$\omega_i(t) = \frac{1}{2 \cdot \max\{V_{m,i}(t), 1\}} \tag{17}$$

Only when the value of $O_i(t)$ is lower then the threshold, $\theta_i(t)$, the source $i$ can receive a backward RM-cell with CI=0 and transmit data at the original transmission rate.

## 5. Simulation Results

Ten MPEG1 frame size traces and synthesized self-similar traffic are utilized herein. The MPEG1 traces, trace1 to trace10, can be found at the ftp site [19]. These frame size traces were extracted from MPEG1 sequences, which have been encoded with the Berkeley MPEG-encoder (version 1.3). Each MPEG video consists of 40,000 frames, which is equivalent to approximately half an hour. The pattern of the MPEG1 stream is IBBPBBPBBPBB, and twenty-four frames are coded per second. The synthesized self-similar streams were generated using a fractional ARIMA (Auto-Regressive Integrated Moving Average) process, which generated a time series with a specified degree of self-similarity $H$.

To determine the network dimensioning, Table 1 lists the mean rate and the peak to mean ratio (P/M) for each trace. To verify the degree of burtiness and self-similarity of each MPEG video trace, the variance coefficient and Hurst parameter are also measured. Tables 2(a) and 2(b) summarize the statistics of MPEG1 and synthesized self-similar traces, respectively. Herein, the variance-time plot technique is applied to estimate the Hurst parameters.

In our simulations, the normalized effective bandwidth for each mechanism is plotted. The desired cell loss rate is set to zero. Figures 5(a)-(c) indicate that using the leaky bucket has the highest normalized effective bandwidths and approaches the peak to mean ratio. However, the curves generated by using MLB with FIR are close to the curves generated by using Norros formula which require the lowest effective bandwidth. Those results further demonstrate that the multiplexing gain exists, even for heterogeneous traffic. This observation also implies that a large amount of bandwidth is wasted when using the conventional leaky bucket mechanism. Therefore, MLB is a preferred option.

This experiment attempts to validate the performance of MLB with FIR when feedback rate regulator and protection policy are applied as well. This experiment is divided into two parts: first, we examine the performance of our simulation model when all input traffic are well-behaving sources. Second, a malicious source is added into the network. Knowing the impact of QoS for each well-behaving source is of relevant interest.

Figures 4(a)-(b) indicate that the CLR drops to zero as long as two or more traffic sources are fed into the MLB. This finding suggests that less bandwidth is needed to achieve the desired cell loss rate when a feedback rate regulator is used. Figures 5(a)-(b) reveal that the MLB with FIR mechanism has the best performance in practice and can reach the upper bound $1/\gamma$, when the number of traffic sources is increased. Each mechanism has the same protection policy. Our proposed mechanism, MLB with FIR traffic prediction, provides the optimum performance in terms of CLR and Delay. The cell loss rates for each well-behaving source drops to zero regardless of whether or not the malicious source is fed.

## 6. Conclusions

This study presents multiple leaky buckets (MLB) with an FIR traffic prediction for the feedback traffic regulator. The proposed mechanism is implemented to monitor and regulate self-similar VBR traffic to avoid congestion. To maximize network utilization, the MLB mechanism integrates all the LBs in the same virtual path. Simulation results demonstrate that the MLB with FIR takes advantage of the statistical multiplexing gain of self-similar VBR traffic. Thus, the MLB with FIR has three to more than ten thousand times cell loss rate improvement than the conventional LB mechanism. To achieve the desired cell loss rate, e.g. CLR=0, the MLB requires a less effective bandwidth than LB and CLB mechanism. Furthermore, the effective bandwidth requirement approaches that estimated by using the Norros formula.

When the resource sharing technique is applied, some other malicious sources must be prevented from degrading the quality of service to established connections. A prominent feature of the malicious source is that its transmission rate is higher than the negotiated mean or peak rate. Reducing the transmission rate is a simple yet effective way.

Simulation results demonstrate that, when the MLB and MLB with FIR traffic prediction and feedback control mechanism are used, a malicious source has difficulty in obtaining extra network resources; the QoS can be maintained for well-behaving sources as well. Our results further demonstrate that using the feedback control mechanism with FIR traffic prediction yields better performance not only for MPEG1 traffic, but also for the data streams with higher self-similarity.

## References


[1] Y. C. Liu and C. Douligeris, "Rate Regulation with Feedback Control in ATM Networks — A Neural Network Approach," *IEEE JSAC*, vol. 15, no. 2, pp. 200-208, Feb 1997.

[2] P. R. Chang and J. T. Hu, "Optimal Nonlinear Adaptive Prediction and Modeling of MPEG Video in ATM Networks Using Pipelined Recurrent Neural Networks," *IEEE JSAC*, vol. 15, no 6, pp.1087-1100, Aug. 1997.

[3] V. Anantharam and T. Konstantopoulos, "Burst Reduction Properties of The Leaky Bucket Flow Control Scheme in ATM Networks," *IEEE Trans. Commun.*, vol. 42, no 12, pp. 3085-3089, Dec. 1994.

[4] F. Bernabei, L. Gratta, M. Listani, A. Sarghmi, "Analysis of ON-OFF Source Shaping for ATM Mutliplexing," *in Proc. of IEEE INFOCOM'93*, pp. 1330-1336, 1993.

[5] T. Konstantopoulos and V. Anantharam, "Optimal Flow Control Schemes That Regulate the Burstiness of Traffic," *IEEE JSAC*, vol. 3, no 4, pp. 423-432, Aug. 1995.

[6] K. Q, Liao, A. Dziong, L. Mason, and N. Tetreault, "Effectiveness of Leaky Bucket Policing Mechanism," *in Proc. of IEEE ICC'92*, pp.1201-1205, 1992.

[7] W. Stallings, "High-Speed Networks: TCP/IP and ATM Design Principles," Prentice-Hall, 1998.

[8] E. P. Rathgeb, "Modeling and Performance Comparison of Policing Mechanisms for ATM Network," *IEEE JSAC*, vol. 9, no. 3, pp. 325-334, Apr. 1991.

[9] H. P. Lin and Y. C. Ouyang, "ATM Cell Discarding Policy by FIR Neural Networks," in Proceeding of IEEE/ICNN97, Houston, U.S.A. vol. 4, pp. 2051-2056, June. 1997.

[10] E. Rumelhart, G. E. Hilton, and R. J. Williams, "Learning representations by backpropagation errors," Nature, vol. 323, pp. 533-536, Oct. 9, 1986.

[11] S. Haykin, "Neural Network A Comprehensive Foundation," Macmillan College

Publishing Company, 1994.

[12] M. Crovella, and A. Bestavros, "Self-similarity in World-Wide Web Traffic: Evidence and Possible Causes," *in Proc. of ACM Sigcomm'96*, May. 1996.

[13] A. Erramilli, O. Narayan, and W. Willinger, " Experimental Queueing Analysis with Long-Range Dependent Packet Traffic," *IEEE/ACM Trans. Networking*, vol. 4, no. 2, pp. 209-223, Apr. 1996.

[14] M. W. Garrett and W. Willinger, "Analysis, Modeling and Generation of Self-similar VBR Video Traffic," *in Proc. of ACM Sigcomm'94*, pp. 269-280, 1994.

[15] K. Park, G. Kim, and M. Crovella, "On the Effect of Traffic Self-similarity on Network Performance," *in Proc. of IEEE SPIE'97*, 1997.

[16] P. Pruthi and A. Popescu, "Effect of Controls on Self-similar Traffic," *in Proc. of the 5th IFIP ATM Workshop*, Jul. 1997.

[17] B. K. Ryu and A. Elwalid, "The Improtance of Long-Range Dependence of VBR Video Traffic in ATM Traffic Engineering: Myths and Realities," submitted to *ACM SIGCOMM '96.*

[18] I. Norros, "On the Use of Fractional Brownian Motion in the Theory of connectionless Networks," *IEEE JSAC*, vol. 15, no. 2, pp. 200-208, Feb 1997.

[19] Available 6: 6-info3.informatik.uni-wuerzburg.de Directory: pub/ MPEG..

[20] J. S. M. Ho, H. Uzunalioglu and I. F. Akyildiz, "Cooperating Leaky Bucket for Average Rate Enforcement of VBR Video Traffic in ATM Networks," *in Proc. of IEEE INFOCOM '95*, pp. 1248-1255, Apr. 1995.

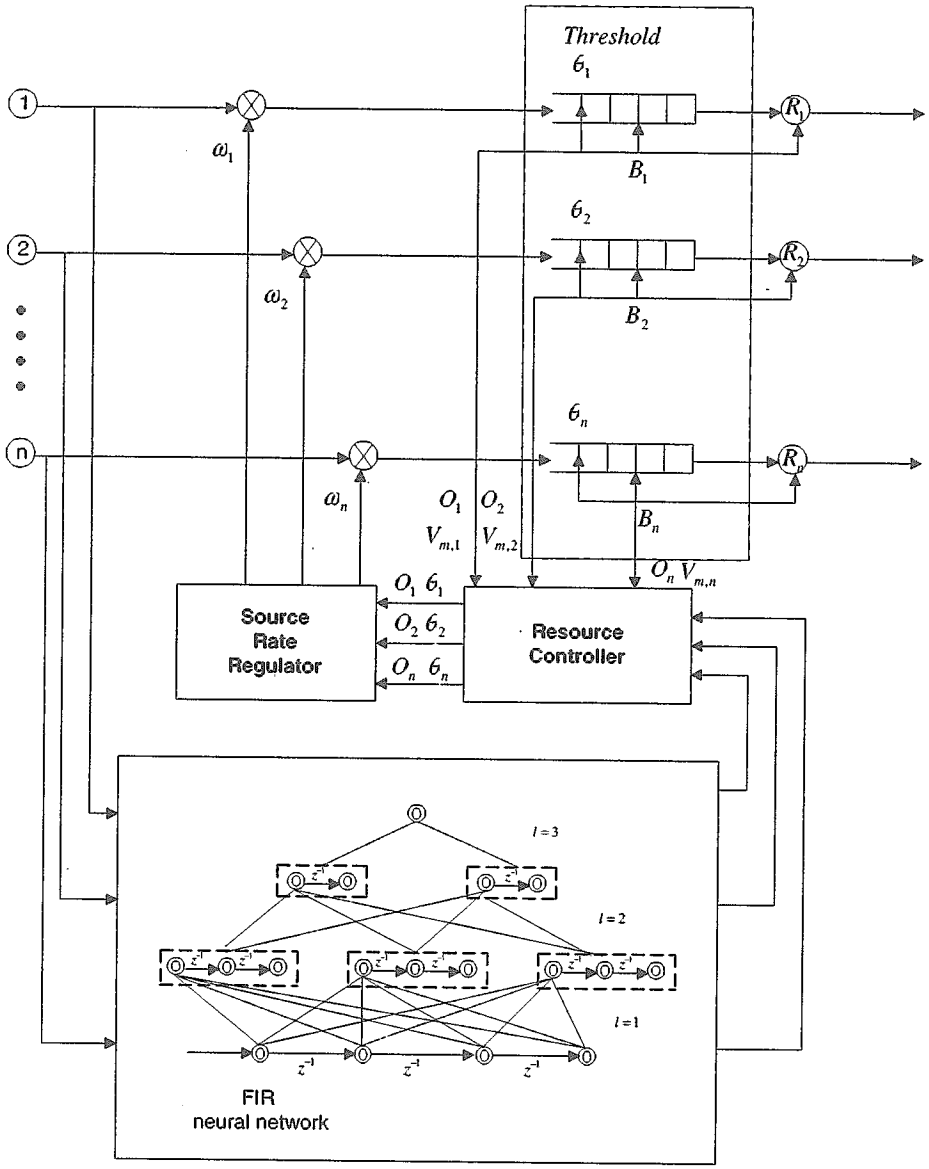


Figure 2 An ATM traffic control model with FIR multilayer neural network using source rate regulator (SRR) on the multiple leaky bucket with buffer sharing.

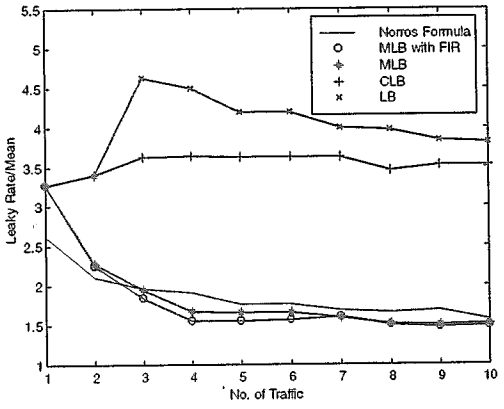


(a)

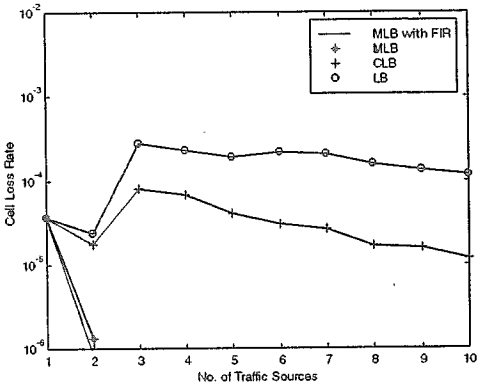


(a)

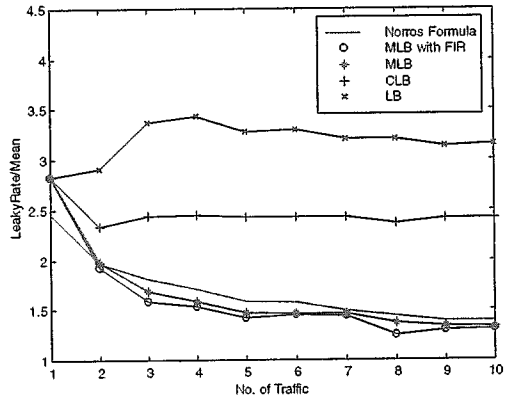


(b)

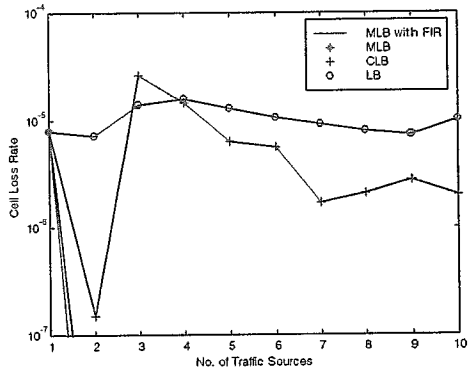


(b)

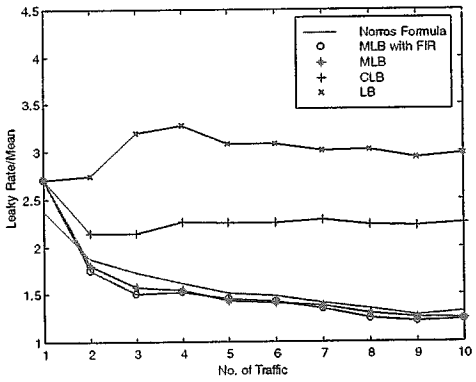


(c)

Figure 3 Normalized effective bandwidth for aggregated MPEG1 traces. (a) $\beta = 0.1$ (b) $\beta = 0.2$ (c) $\beta = 0.3$

Figure 4 Cell loss rate for aggregated traffics using feedback control mechanism. (a) MPEG1 traces, $\gamma = 1.3$, $\beta = 0.1$ (b) Synthesized self-similar data series,

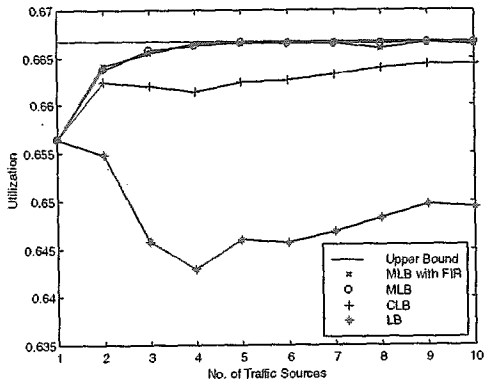


(a)

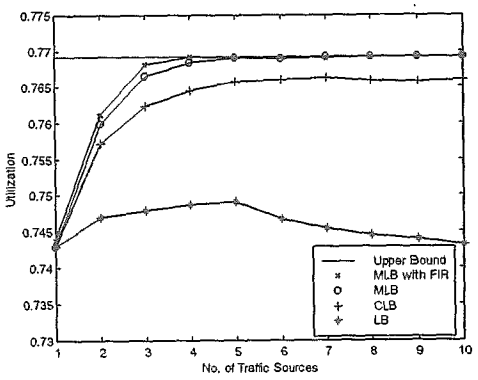


(b)

Figure 5 Utilization for aggregated traffics using feedback control mechanism.(a) MPEG1 traces, $\gamma = 1.3$, $\beta = 0.1$ (b) Synthesized self-similar data series, $\gamma = 1.2$ $\beta = 0.1$ .

Table 1 Statistics of input traffic for (a) MPEG1 traces.

| Traces No. | Name of Video | Frames | | Bit rate | | $a$ | $H$ |
|---|---|---|---|---|---|---|---|
| | | Mean (Kbits/Frame) | P/M | Mean (Kbits/sec) | P/M | | |
| trace1 | Goldfinger | 24.3 | 10.1 | 569.7 | 3.12 | 77648 | 0.85 |
| trace2 | Dino | 13.1 | 9.1 | 306.5 | 3.49 | 46907 | 0.76 |
| trace3 | Lamb | 7.3 | 18.4 | 171.4 | 4.70 | 61045 | 0.81 |
| trace4 | StarWars | 15.6 | 11.9 | 218.3 | 3.80 | 69831 | 0.83 |
| trace5 | Terminator II | 10.9 | 7.3 | 255.6 | 2.53 | 26276 | 0.72 |
| trace6 | Movie preview | 14.3 | 12.1 | 334.9 | 3.40 | 76685 | 0.74 |
| trace7 | ATP final | 21.9 | 8.7 | 513.0 | 2.78 | 67297 | 0.71 |
| trace8 | Race | 30.7 | 6.6 | 720.7 | 3.37 | 91797 | 0.76 |
| trace9 | Super bowl | 23.5 | 6.0 | 550.9 | 2.68 | 71035 | 0.78 |
| trace10 | Soccer | 25.1 | 7.6 | 588.5 | 3.66 | 131266 | 0.80 |

(a)

(b) Synthesized self-similar data series

| Traces No. | Mean (Kbits/sec) | P/M | $a$ | $H$ |
|---|---|---|---|---|
| trace1 | 428.6 | 2.64 | 52341 | 0.81 |
| trace2 | 443.1 | 2.29 | 43306 | 0.81 |
| trace3 | 425.3 | 2.25 | 47189 | 0.82 |
| trace4 | 425.3 | 2.71 | 42966 | 0.84 |
| trace5 | 400.6 | 2.60 | 37991 | 0.84 |
| trace6 | 484.2 | 2.67 | 81664 | 0.85 |
| trace7 | 406.5 | 3.16 | 64304 | 0.85 |
| trace8 | 594.0 | 2.81 | 84140 | 0.89 |
| trace9 | 452.1 | 2.38 | 66310 | 0.88 |
| trace10 | 358.9 | 3.24 | 61147 | 0.89 |

(b)